frontiers | Frontiers in Materials

TYPE Original Research
PUBLISHED 28 October 2024
DOI 10.3389/fmats.2024.1473032

OPEN ACCESS

EDITED BY
Egemen Avcu,
Kocaeli University, Türkiye

REVIEWED BY
Mustafa Armağan,
Istanbul Medeniyet University, Türkiye
Nida Iqbal,
University of Engineering and Technology, Lahore, Pakistan
Eray Abakay,
Sakarya University, Türkiye

*CORRESPONDENCE
Hussein Alrobei,
H.alrobei@psau.edu.sa

RECEIVED 30 July 2024
ACCEPTED 30 September 2024
PUBLISHED 28 October 2024

CITATION
Imran A, Malik RA, Alrobei H and Ur Rehman MA (2024) Electrophoretic deposition of polyetheretherketone/polytetrafluoroethylene on 316L SS with improved tribological and corrosion properties for biomedical applications.
Front. Mater. 11:1473032.
doi: 10.3389/fmats.2024.1473032

Electrophoretic deposition of polyetheretherketone/polytetrafluoroethylene on 316L SS with improved tribological and corrosion properties for biomedical applications

Ayman Imran[1], Rizwan Ahmed Malik [2], Hussein Alrobei[2]* and Muhammad Atiq Ur Rehman[1,3]

[1]Centre of Excellence in Biomaterials and Tissue Engineering, Materials Science Engineering Department, Government College University, Lahore, Pakistan, [2]Department of Mechanical Engineering, College of Engineering, Prince Sattam bin Abdulaziz University, Al-kharj, Saudi Arabia, [3]Department of Materials Science and Engineering, Institute of Space Technology Islamabad, Islamabad, Pakistan

Introduction: 316L stainless steel (316L SS) has poor wear and corrosion resistance compared to that of the Cp-Ti and Ti-6Al-4V implants [when studied under a physiological environment using phosphate-buffered saline (PBS)]. However, 316L SS implants are cost-effective. Their wear and corrosion properties can be improved by depositing biocompatible coatings.

Method: In this research work, a polymer coating of polyetheretherketone (PEEK) and polytetrafluoroethylene (PTFE) was deposited at optimized parameters (20 V for 3 min) on 316L SS via electrophoretic deposition (EPD). We compared the performance between of the PEEK coating and hybrid PEEK/PTFE coatings for biomedical applications. The PEEK/PTFE coating was sintered at 350°C for 30 min.

Results and Discussion: Scanning electron microscopy (SEM) analysis revealed that the PEEK/PTFE coating showed a uniform coating with a uniform thickness of ~80 µm. Fourier transform infrared (FTIR) spectroscopy analysis confirmed the presence of bonds attributed to the PEEK and PTFE coatings. The PEEK/PTFE coating exhibited adequate average surface roughness (R_a) of 2.1 $\pm$ 0.2 µm with a high value of contact angle of 132.71 $\pm$ 3, indicating the hydrophobic nature of the PEEK/PTFE coating. Scratch tests evaluated that the PEEK/PTFE coating demonstrated a 7 N load, which indicated the good adhesion between the coating and 316L SS. Furthermore, the PEEK/PTFE coating demonstrated good wear resistance, capable of withstanding a 7 N load under dry conditions, and showed a specific wear rate of ~0.0114 mm^3/Nm. Electrochemical analysis conducted using the phosphate-buffered saline (PBS) solution demonstrated that the corrosion rate of 316L SS was reduced from 0.9431 mpy to 0.0147 mpy by depositing the PEEK/PTFE

coating. Thus, the developed coatings present suitable wear and corrosion resistance and are thus considered for potential orthopedic applications.

KEYWORDS

polytetrafluoroethylene, polyether ether ketone, electrophoretic deposition, corrosion-resistant coatings, wear-resistant coatings

1 Introduction

Metallic implants made of AISI 316L stainless steel (316L SS) and titanium are used for orthopedic applications (Batool et al., 2021). Titanium implants offer superior wear and corrosion resistance, but their high cost is a notable disadvantage compared to 316L stainless steel (SS) implants (Atiq Ur Rehman et al., 2017). Poor wear and corrosion resistance of 316L SS implants compared to those of Cp-Ti and Ti-6Al-4V implants can result in the uncontrolled release of toxic ions (Ni and Cr) in the human physiological fluid (Rehman and Batool, 2022).

Orthopedic implants are used to restore the body's natural function. The common cause of failure of orthopedic implants includes infection (due to wear debris, release of toxic ions, and biofilm formation), loosening of the implant due to stress shielding, and poor osseointegration due to the mismatch in the surface chemistry of the implant and physiological environment (Moskalewicz et al., 2013; Moskalewicz et al., 2018; Nawaz et al., 2021). Thus, it is imperative to control implant-associated infections and tune the surface of 316L SS to improve the wear and corrosion resistance (corrosion resistance will help prevent the release of toxic ions from the metallic substrate). Implant-associated infection can be controlled through application of antibacterial coatings (Simchi et al., 2011; Ur Rehman et al., 2020), including metallic ions/natural herbs (Pishbin et al., 2013; Pishbin et al., 2014; Ballarre et al., 2020), which can prevent the formation of biofilms. Furthermore, the implant should be biocompatible to promote the attachment of osteoblast cells (Nawaz et al., 2023; Nawaz et al., 2024).

Electrophoretic deposition (EPD) is a promising method for depositing coatings in which binders are not needed (Ahmed et al., 2020; Atiq Ur Rehman et al., 2020). It is a colloidal process in which materials can be deposited by the application of DC (Baştan et al., 2018). It is the most appropriate and cost-effective process in which the desired materials can be deposited by using low solid content (Besra and Liu, 2007). It offers excellent control of the thickness, stoichiometry, and microstructure of the deposited layers by suitably adjusting the applied voltage and treatment time (Boccaccini et al., 2010). By adjusting the deposition time and voltage, excellent control of the microstructure, thickness, and stoichiometry is achieved. EPD involves two processes: electrophoresis and deposition (Batool et al., 2021). Electrophoresis involves the movement of particles under the influence of an electric field. In the second step, the particles are deposited in the form of a dense mass (Besra and Liu, 2007; Ferrari and Moreno, 2010; Avcu et al., 2019). Polytetrafluoroethylene (PTFE) is a synthetic fluoropolymer that is synthesized from fluorspar (calcium fluoride), chloroform, and hydrofluoric acid by a complex series of reactions involving pyrolysis and fluorination. PTFE has a wide range of industrial applications (Armağan and Arıcı, 2021). Owing to the high melting point, PTFE is chemically stable against many solvents and solutions. It is also a biocompatible polymer like PEEK (Yuan and Yang, 2010). It is thermoplastic and has excellent abrasive and chemical resistance. It has a low coefficient of friction and is highly resistant to corrosion (Dhanumalayan and Joshi, 2018). PTFE has excellent sliding properties, so it has been used in many engineering applications. It is also used as a self-lubricating material. PTFE has low wear resistance and demonstrates poor adhesion to substrates (Armağan and Arıcı, 2021), so PTFE cannot be used alone in coating. PTFE coatings were deposited on the AZ31 alloy by EPD, and charge transfer resistance was increased (Xiang et al., 2022).

Polyetheretherketone (PEEK) is a high-engineering performance synthetic thermoplastic polymer. PEEK is semi-crystalline and highly resistant to heat and chemicals (Panayotov et al., 2016). The biomechanical properties of PEEK are close to those of the bone; thus, PEEK is widely accepted as an implant material. PEEK reduces the stress-shielding effects of bone, and hence the chances of bone resorption and osteolysis are reduced. Ahmad et al. (2023a) deposited PEEK coatings on 316L SS, which showed good wear and improved corrosion resistance.

Ur Rehman et al. (2020) deposited the PEEK/bioactive glass (BG) coating on 316L SS to achieve high corrosion resistance, wear resistance, and bioactivity. To gain antibacterial properties, another layer of chitosan/lawsone/BG was deposited on the PEEK/BG layer, and a controlled release of lawsone was achieved. PEEK/PTFE coatings were deposited on Ti-6Al-4V by EPD to improve scratch resistance and wear resistance (Fiołek et al., 2020b). Zhang et al. (2023a) deposited the PTFE coating on AZ31 alloys, and the corrosion current density was reduced remarkably. Thus, electrophoretic sintered PTFE coatings can significantly improve the charge transfer resistance. In another study (Ur Rehman et al., 2020), PEEK/BG coatings were deposited on 316L SS and sintered at 400°C to achieve high bioactivity and improved wear and corrosion resistance.

Chen et al. (2020) deposited PEEK and PTFE coatings to control the wear of an implant. Fiołek et al. (2020a) deposited PTFE/PEEK coatings on Ti implants by EPD and employed the sintering process to improve the adhesion strength of the coating and also investigated the tribological properties of the coating. Song et al. (2016) deposited different PEEK-based composite coatings consisting of PEEK/alumina and PEEK/silica on Ti6Al4V to modify its surface. These PEEK-based composite coatings were characterized in terms of their wear and corrosion resistance.

De Riccardis et al. (2013) deposited the PEEK/PTFE coating on 316L SS via EPD. However, in the current study, a novel approach of incorporating a newly designed sintering process of PEEK/PTFE coatings was introduced. This innovative approach significantly improved the wear and corrosion resistance of 316L SS by depositing the PEEK/PTFE coating. In this study, the author deposited PEEK coatings on 316L SS via EPD and characterized its desired properties

in terms of wear and corrosion resistance. The tribological study showed that PEEK coatings can withstand a load of 7 N load (in dry sliding conditions) along with a high specific wear rate of ~0.0961 mm^3/Nm and a corrosion rate of ~0.067 mils per year (mpy). However, after the incorporation of PTFE particles in the PEEK coating and sintering at 350°C, the specific wear rate was significantly decreased from ~0.0961 to 0.0114 mm^3/Nm, while the corrosion rate of 316L SS after the PEEK/PTFE coating also decreased from ~0.067 to 0.014 mpy (mean improved corrosion resistance). Thus, the PEEK/PTFE coating has the potential to improve the implant's performance. Herein, the authors reported improved corrosion and wear resistance of the PEEK/PTFE coating when compared to the previous literature. Thus, this study is a step forward for PEEK-based composite coatings to be considered for clinical applications. Finally, the successful development of a polymeric coating system through the newly developed heating cycle was also studied in terms of the wear and corrosion resistance of 316L SS-based biomedical implants.

Future research on PEEK/PTFE coatings will focus on *in vivo* studies, which are essential for long-term performance and efficiency in terms of improved wear and corrosion resistance of 316L SS implants after deposition of PEEK/PTFE coatings.

2 Materials and methods

PTFE (1 µm size), absolute ethanol, and chitosan powder were purchased from Sigma-Aldrich. The 316L SS sheet was used to prepare the PEEK/PTFE coating substrates. The composition of 316L SS was Cr-16.5%, Ni-10%, Mo-2%, N-0.10%, S-0.015%, P-0.045, C-0.03, Si-1.00%, Mn-2.00%, and Fe (balance %) (Ali et al., 2022). PEEK powder (10 µm) was purchased from Vitrex, United Kingdom (Heavens, 1990).

2.1 Methods

2.1.1 Sample preparation

A shear cutter was used to cut a 3 × 1.5 cm^2 316L SS sheet. The cleaning of substrates was done using acetone and ethanol at the ratio 1:1. The samples were ultrasonicated for 10 min, rinsed in distilled water, and subsequently dried in air.

2.1.2 Suspension preparation of PEEK

First, a chitosan solution was prepared by dissolving 0.5 g/L of chitosan in the solution of 1 vol% acetic acid and 20 vol% distilled water and magnetically stirred for 30 min. Afterward, 79 vol% ethanol was added to the prepared solution; details can be found elsewhere (Atiq et al., 2019). The addition of ethanol prevented the hydrolysis of water during the EPD process. It is important to note that a 0.5 g/L concentration of chitosan was chosen based on the suspension stability because if a higher concentration of chitosan is used, it may result in inhomogeneous coatings (Avcu et al., 2018; Atiq et al., 2019). A stable suspension of 0.5 g of PEEK in 50 mL chitosan solution was prepared by stirring for 15 min on a magnetic stirring plate and, subsequently, ultrasonicated for 15 min; this process was repeated two times, and the pH of the suspension was checked.

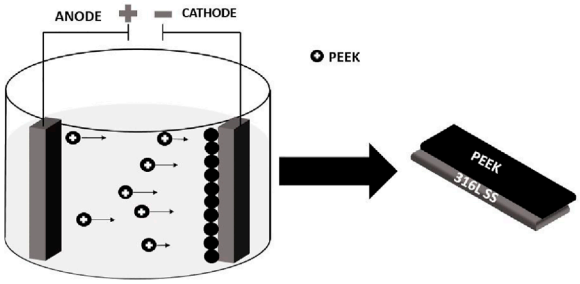

FIGURE 1
Schematic representation of cathodic EPD in which PEEK particles are deposited on the cathode.

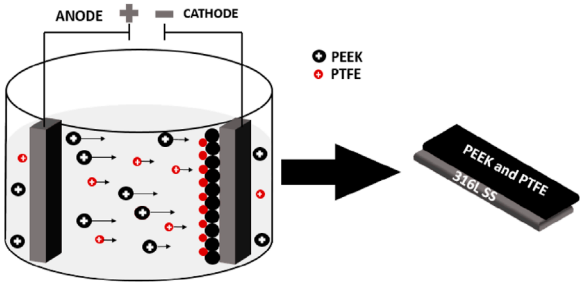

FIGURE 2
Schematic representation of cathodic EPD in which positively charged PEEK/PTFE particles were deposited on the cathode.

2.1.3 Electrophoretic deposition of PEEK and PEEK/PTFE

A stable suspension of PEEK was prepared in a chitosan solution where PEEK particles were positively charged. The macromolecules of chitosan are absorbed at the surface of PEEK particles and impart a positive charge. The 316L SS substrates were immersed in the stable suspension for deposition. As the potential of 15 V with 3 min was applied to the suspension, positively charged PEEK particles were deposited on the negatively charged electrode (cathode) (Avcu et al., 2018). Under the acidic pH of ~4.17, the protonation of the amine groups of chitosan resulted in the adsorption of these groups on the surface of PEEK particles in the suspension. Figure 1 shows the schematic representation of cathodic EPD of PEEK particles under an applied potential of 15 V with 3 min deposition time.

To deposit the PEEK/PTFE coating, a mixture of 3 g/L PEEK and 1 g/L PTFE was added to 50 mL of the chitosan solution, magnetically stirred for 20 min, and then ultrasonicated for 30 min. This process was also repeated twice. Finally, the PEEK/PTFE suspension was stirred for 10 min, and the pH was set at 4.5 through the dropwise addition of acetic acid, which assisted in forming a stable suspension.

A stable suspension of PEEK/PTFE was subjected to cathodic deposition on 316L SS substrates. 316L SS substrates were immersed in the stable suspension of PEEK/PTFE for deposition. As the electric field of 20 V/cm with 3 min was applied, positively charged PEEK and PTFE particles were deposited on the negatively charged electrode (cathode). Under the acidic pH ~ 4.5, the protonation of

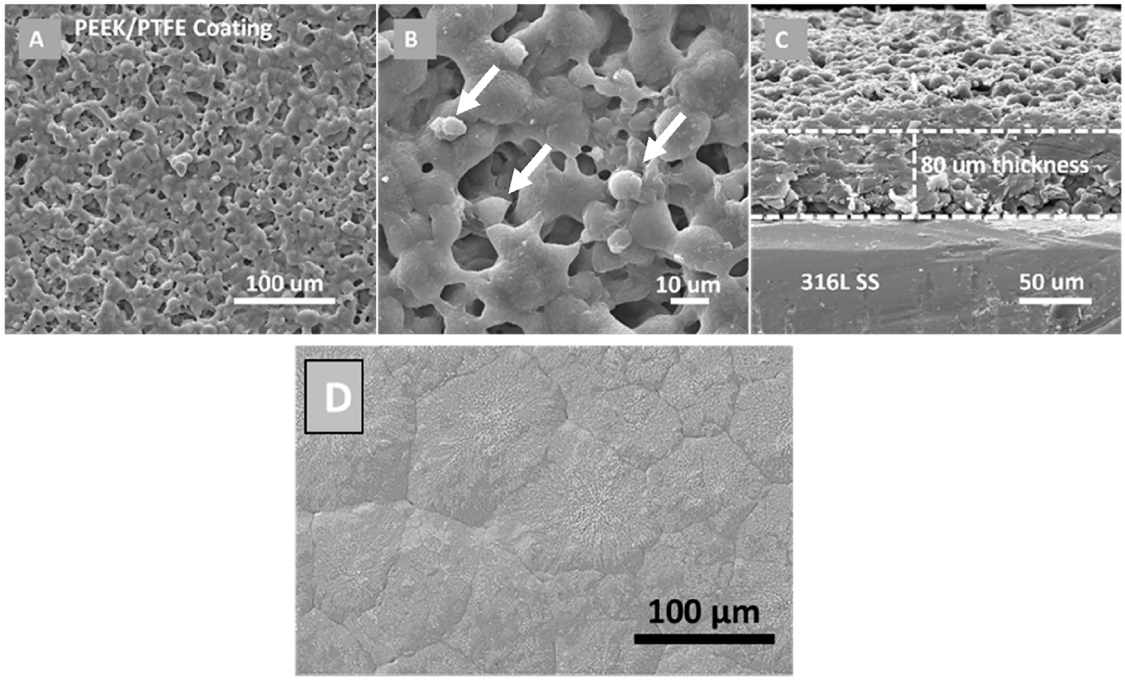

FIGURE 3
SEM images of PEEK/PTFE coatings deposited on 316L SS via EPD at optimized parameters: **(A)** lower magnification image at the surface, **(B)** higher magnification image at the surface, **(C)** cross-sectional image; and **(D)** SEM image of PEEK coatings deposited on 316L SS via EPD and sintered at 350°C [adopted from (Ahmad et al., 2023a) with permission from Elsevier].

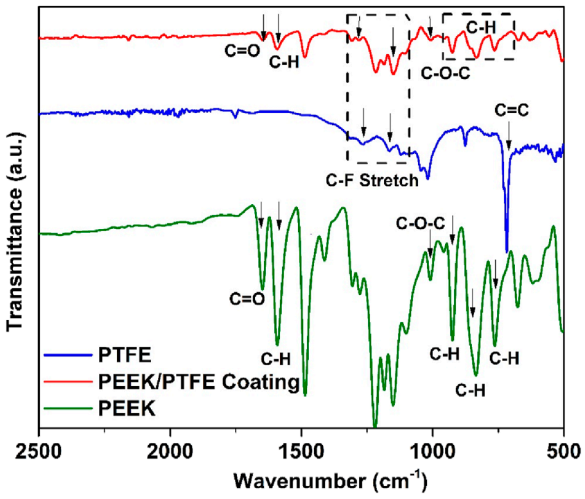

FIGURE 4
FTIR spectra of PEEK, PTFE, and PEEK/PTFE composite coating.

the amine groups of chitosan resulted in the adsorption of these groups on the surface of PEEK/PTFE particles, imparting a net positive charge to each particle in the suspension. Figure 2 shows the schematic representation of cathodic EPD of PEEK/PTFE coatings.

After the deposition of PEEK coating and PEEK/PTFE coating on 316L SS at an area of 2.25 cm^2, these coatings were sintered at 350°C for 30 min at a heating rate of 10°C/min in the box furnace (KSL-1700X-A7). The sintering of the coating at 350°C resulted in a change in color from white to brown.

On visual inspection, it looked like PEEK and PTFE particles were fused. Furthermore, these sintered coatings were subjected to different characterization techniques like morphological analysis by scanning electron microscopy (SEM) and Fourier transform infrared spectroscopy (FTIR) to identify functional groups, surface properties by contact angle, and roughness measurement. These coatings were also subjected to a scratch test to evaluate the adhesion of the coatings with 316L SS. Furthermore, the electrochemical and wear resistance properties of the coatings were investigated by potentiodynamic polarization, electrochemical impedance spectroscopy, and tribological testing. We performed a comparative study between the properties of PEEK and PTFE/PTFE coatings.

2.1.4 Characterization of coatings

2.1.4.1 Morphological analysis of PEEK/PTFE coating (SEM analysis)

The morphological analysis and cross-sectional analysis of coating were carried out by SEM (Auriga 219 4750 from Carl Zeiss, Germany). Before taking SEM images, the samples were sputtered with gold–palladium (Au/Pd) to enhance the images' quality and reduce charging effects. The thickness of the sputtering was approximately 5 nm. In the SEM images, primary electrons interacted with the surface of the PEEK/PTFE coating and ejected the low-energy electrons (secondary electrons), which generated the coating's topographical image.

TABLE 1 Characteristics of FTIR bands of PEEK, PTFE, and PEEK/PTFE coating deposited on 316L SS via EPD.

Wavenumber (cm^{-1})	Corresponding bond	Associated material	Reference
762, 834, and 924	C–H aromatic rings	PEEK and PEEK/PTFE	Baştan et al. (2018)
1,590	C–H angular deformation	PEEK	de Sá et al. (2021)
1,648 and 1,006	C=O C–O–C	PEEK and PEEK/PTFE PEEK and PEEK/PTFE	Atiq Ur Rehman et al. (2017) Atiq Ur Rehman et al. (2017)
1,280, 1,163, and 668	C–F Stretch	PTFE	Mahmoud Nasef et al. (2013) Wang et al. (2018)
1,282 and 1,147	C–F Stretch	PEEK/PTFE	Mahmoud Nasef et al. (2013) Wang et al. (2018)

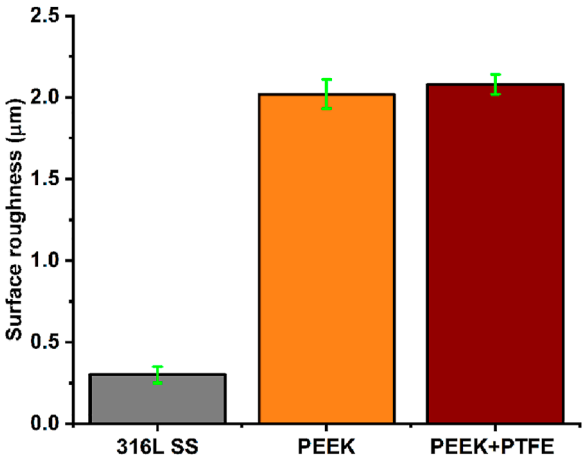

FIGURE 5
Average surface roughness value (Ra) of bare 316L SS, PEEK, and PEEK/PTFE coating. Error bars indicate the standard deviation where n = 5.

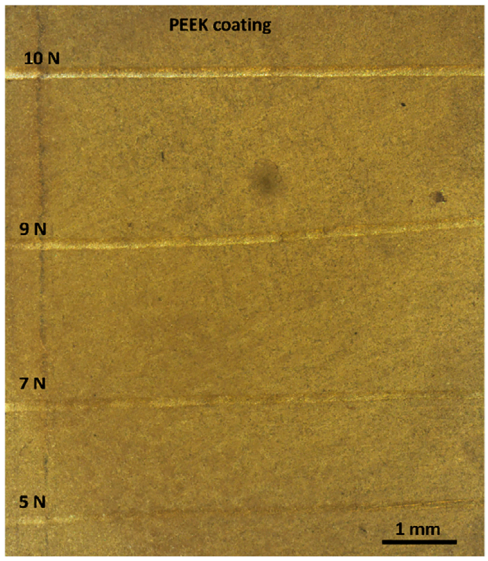

FIGURE 6
Shows the scratch test to evaluate the adhesion strength of PEEK coatings deposited on 316L SS via EPD.

2.1.4.2 Functional group identification (FTIR analysis)

The functional groups of PEEK and PTFE were identified via attenuated total reflection (ATR)–FTIR (Nicolet 6700 device from Thermo Scientific) spectroscopy, in the wavelength of 2,500–500 cm^{-1} at a resolution of 4 cm^{-1}. The FTIR results were analyzed by using the OMNIC paradigm software. The transmittance mode was used to conduct the FTIR analysis.

2.1.4.3 Surface roughness

The average surface roughness (R_a) of coatings and 316L SS was measured using a contact-type profilometer (TMR 360). The diamond stylus touched the surface of 316L SS and coatings to calculate the values of R_a. When the diamond-tipped stylus moved 5 mm back and forth along a straight line on 316L SS and coatings, the stylus traversed the surface and followed the contour, and a profilometer was used to record this movement of the stylus. The built-in profilometer software calculated the Ra of the coating and the bare 316L SS.

2.1.4.4 Contact angle

ImageJ software measured the values of CA of coatings and 316L SS. First, a droplet of 5 µL of distilled water was dispensed in a spherical shape using a 100-µL pipette on the surface of PEEK and PEEK/PTFE coatings deposited on 316L SS. The photographs of the droplet were taken using the digital camera after 5 s of dispensing on the surface of the layer and 316L SS. These photographs were imported into the software, and the values of contact angles were measured.

2.1.4.5 Scratch test

The scratch test determined the adhesion strength and mechanical properties of PEEK and PEEK/PTFE coatings deposited on 316L SS. The scratch test gave an insight into the ability of coatings to withstand mechanical stresses during implantation and usage in the human body. A 10-mm tungsten carbide hemispherical stylus of the automatic scratch tester (BEVS 2801, China) produced a

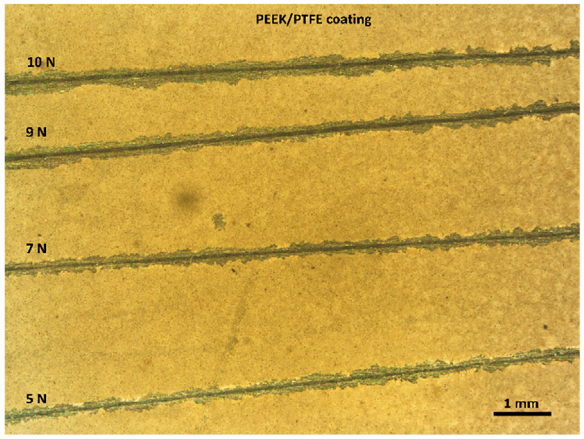

FIGURE 7
Shows the scratch test conducted to evaluate the adhesion strength of PEEK/PTFE coatings deposited on 316L SS via EPD.

linear scratch on the surface of the coating. A progressive load of 5, 7, 9, and 10 N was applied sequentially to calculate the critical load (the load at which the coating failed or delaminated from the 316L SS [10].

2.1.4.6 Electrochemical studies

Electrochemical studies of potentiodynamic polarization (PDP) and electrochemical impedance (EIS) analyses were carried out to investigate the barrier properties of PEEK, PEEK/PTFE coatings, and 316L SS. A potentiostat (Gamry Reference 600) consists of a three-electrode system that acts as a working Ag/AgCl reference and graphite counter electrode. The open circuit potential (OCP) was determined for the first 60 min. The EIS of the coating and 316L SS was determined in the frequency range of 0.01 Hz–10^6 Hz and 10 mV as AC perturbation. The Gamry instrument measured the resulting AC response from the coating and 316L SS. The EIS data were analyzed using ZSimpWin software) for fitting. Finally, PDP was also performed. All polarization scans were determined at 37°C ± 2°C at the 0.5 mV/s scan rate in the potential range of ±1.5 V. All the electrochemical analyses were carried out using phosphate-buffered saline (PBS) as an electrolyte to mimic the human physiological environment. The PDP data were analyzed using CorrView software to calculate the corrosion potential (E_{corr}), corrosion current density (i_{corr}), and corrosion rates of the deposited coatings and bare 316L SS.

2.1.4.7 Tribological study

The wear resistance of PEEK and PEEK/PTFE coatings was measured via the tribological test. A tribometer (MT/60/NI, Spain) and pin-on-disc test are standard tests to evaluate the wear resistance of PEEK and PEEK/PTFE coatings. Various normal loads ranging from 1 N to 9N with the increase in load of 2 N were applied on PEEK and PEEK/PTFE coatings. However, the results of the maximum load of 7 N showed that PEEK and PEEK/PTFE coatings exhibited comparable wear resistance. The normal applied load is 9N, at which the coatings delaminated during the pin-on-disc test. The wear behavior of PEEK and PEEK/PTFE coatings at 7N was investigated. The specific wear rates of PEEK and PEEK/PTFE coatings were calculated using Equation 1.

$$\text{Specific wear rate} = \frac{\text{Cumulative wear volume}}{\text{applied load} \times \text{Sliding distance}}. \quad (1)$$

However, the cumulative wear volume was calculated from the tribological test data sheet.

Following our studies, the wear test was conducted under dry sliding conditions at room temperature on PEEK and PEEK/PTFE coatings (Ur Rehman et al., 2020; Ahmad et al., 2023a). The wear resistance of PEEK and PEEK/PTFE coatings was computed in terms of a specific wear rate.

3 Results and discussion

3.1 Morphological analysis of the PEEK/PTFE coating (SEM analysis)

The SEM images of the PEEK/PTFE coating at high and low magnification revealed that the coating is uniform, in which PTFE particles are uniformly infused into the PEEK matrix after sintering the PEEK/PTFE coating at 350°C for 30 min (Figures 3A, B). It is assumed that the infusion is due to the capillary action during sintering. No agglomerates of PTFE particles were observed in the PEEK/PTFE coating. It appeared that PEEK/PTFE completely covered the 316L SS substrate. Figure 3C illustrates the cross-sectional view of the PEEK/PTFE coating, revealing the coating thickness of ~80 µm. Figure 3D shows the SEM image of the PEEK coating deposited on 316L SS via EPD and later sintered at 350°C.

The white arrows marked in the PEEK/PTFE coating can potentially be PTFE. When we compared the SEM image of the PEEK coating with the PEEK/PTFE coatings, we observed that the small globules are an additional feature in the PEEK/PTFE coating.

3.2 Functional group identification (FTIR spectroscopy)

The ATR–FTIR spectra of PEEK, PTFE, and PEEK/PTFE coatings are presented in Figure 4. The characteristic aromatic ring (C–H) bands in PEEK were identified at 762, 834, and 924 cm^{-1}. The ether linkage (C–O–C) and carbonyl (C=O) stretching vibrations were observed at 1,006 and 1,648 cm^{-1}, respectively. The band at 1,590 cm^{-1} corresponded to the angular deformation of the C–H bond. The FTIR results of PEEK in this study are consistent with those of the literature (Atiq Ur Rehman et al., 2017; Baştan et al., 2018). In the FTIR spectra of PTFE, strong bands attributed to the C–F bond were observed between 1,000 and 1,300 cm^{-1}. Specifically, the CF_2 asymmetrical and symmetrical stretching bands and the weak CF2 wagging bands appeared at 1,280, 1,163, and 668 cm^{-1}, respectively. The FTIR results of PTFE are consistent with those of the literature (Mahmoud Nasef et al., 2013; Wang et al., 2018; de Sá et al., 2021).

The FTIR spectra of the PEEK/PTFE coating confirmed the consolidation of PTFE particles in the PEEK matrix. The characteristic CF_2 bands in the composite coating exhibited slight shifts, appearing at 1,282 and 1,147 cm^{-1}. The bands corresponding

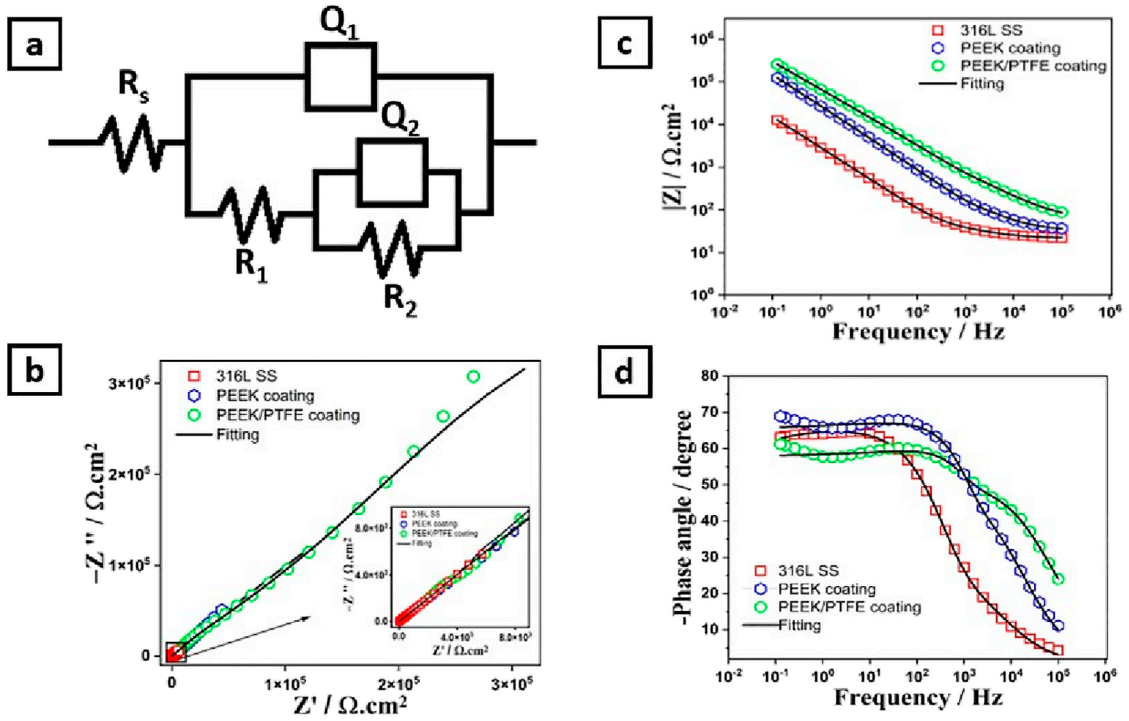

FIGURE 8
(A) Shows the electrical equivalent circuits of 316L SS, PEEK, and PEEK/PTFE coating, **(B)** Nyquist plot, **(C)** Bode impedance plot, and **(D)** Bode phase angle plots.

TABLE 2 Illustrates the values of the equivalent circuit fitting EIS spectra acquired on bare 316L SS and PEEK and PEEK/PTFE coatings.

Sample	R_s	Q_1	n_1	R_1	Q_2	n_2	R_2	Chi-squared
	(Ω cm^2)	($\mu\Omega^{-1}$ s^n cm^{-2})	—	(kΩcm^2)	($\mu\Omega^{-1}$ s^n cm^{-2})	—	(kΩcm^2)	
316L SS	21	70	0.6	320	22	0.8	0.036	1.66e-4
PEEK coating	32	9.2	0.8	400	0.4	0.8	0.31	4.48e-4
PEEK/PTFE coating	56	1.4	0.4	2,400	1	0.8	4.2	3.18e-3

to the C=O, C–O–C, and C-H of PEEK also appeared in the composite coating at 1,648, 1,008, and 1,590, respectively. The FTIR results of PEEK/PTFE coatings are in agreement with those of Mahmoud Nasef et al., 2013; Atiq Ur Rehman et al., 2017; Baştan et al., 2018; Wang et al., 2018; de Sá et al., 2021).

The summary of all bands identified is given in Table 1, which illustrates the FTIR spectra of PEEK, PTFE, and PEEK/PTFE coatings.

3.3 Surface roughness

Roughness is critical in the surface modification of 316L SS implants via coatings. The coating material's nature alters the surface properties of the implant, which significantly affects the performance of the implant (Ureña et al., 2018; Ballarre et al., 2020). The surface roughness has a significant impact on protein and cell attachment. The osteoblast cells prefer surface roughness in the range of 1–2 µm (Nawaz et al., 2020). Roughness measurements in Figure 5 show that 316L SS, PEEK, and PEEK/PTFE exhibited R_a values of 0.3 ± 0.05 µm, 2.02 ± 0.09 µm, and 2.08 ± 0.06 µm, respectively. Similar values of R_a coatings have been reported in the literature for the preferred osteoblast-like cell attachment (Ureña et al., 2018; Wennerberg, 1999). It is essential to mention that the roughness alone cannot confirm the suitability of the implant for a positive cellular interaction. It is necessary to study the wettability and surface chemistry to determine the suitability of an implant for orthopedic applications. PEEK/PTFE coatings tailored the R_a values of 316L SS in the preferred range, thus establishing the suitability of the coatings for orthopedic applications.

To facilitate the attachment of osteoblast cells, several events should occur, for example, surface recognition, development of initial contacts, and focal contacts (involves interactions of

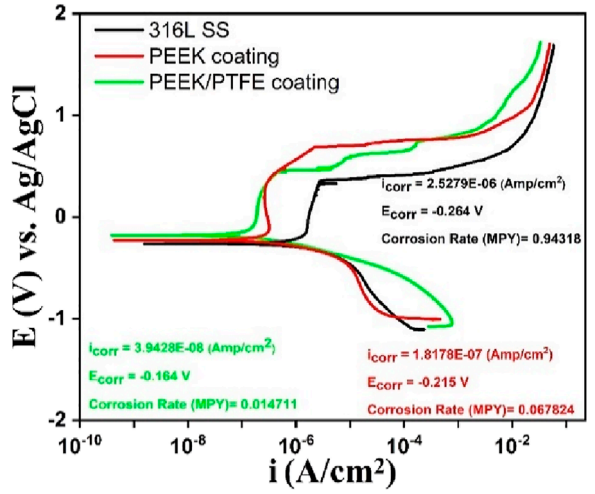

FIGURE 9
Potentiodynamic polarization scans of 316L SS, PEEK coating, and PEEK/PTFE coating deposited on 316L SS via EPD.

integrins-Arg-Gly-Asp- and extracellular matrix proteins such as fibronectin), followed by the spreading of osteoblasts which govern the shape of the cell. Thus, precise control over surface roughness can provide twofold advantages, such as favorable attachment and proliferation of osteoblasts and resisting the adhesion of bacteria (Celles and dos Reis, 2024). Later, the proliferation rate will determine the speed (of bone formation), density, and quality of the bone (Matsuura et al., 2024). Accordingly, it can be hypothesized that the favorable roughness of PEEK/PTFE coatings can support the regeneration of bone, thus confirming the suitability of the PEEK/PTFE coating for orthopedic applications.

3.4 Contact angle

The nature of the surfaces of 316L SS, PEEK coating, and PEEK/PTFE coating was evaluated via contact angle measurement. The contact angle value of 316L SS was 78.06° ± 2°, which increased to 82.90° ± 1.5° upon deposition of the PEEK coating. The addition of PTFE in PEEK increased the contact angle value to 132.71° ± 3°. Thus, the hydrophobic characteristic is imparted to the developed coating. Cellular attachment is a crucial factor for an implant surface, and it depends upon the nature of the surface, whether the surface is hydrophilic or hydrophobic. To achieve anticorrosive properties, the orthopedic implants should be hydrophobic (Zhang et al., 2023b). Recently, hydrophobic surfaces have been reported to exhibit anticorrosive properties. This can be because hydrophobicity can slow down the transportation of water and corrosive ions in coatings (Chen et al., 2009). In the atmospheric environment, the microstructure on the hydrophobic surface can capture a lot of air, effectively decreasing the contact area between water and the hydrophobic surface. Thus, a hydrophobic surface can prevent atmospheric corrosion by impeding the formation of the electrolyte film (Wang et al., 2013). In an immersion environment, the air film on a hydrophobic surface can temporarily act as a physical barrier that improves corrosion resistance (Xu et al., 2021).

3.5 Scratch test

Scratch tests were conducted to evaluate the adhesion strength of the PEEK/PTFE coating and compare it with that of the PEEK coating deposited on 316L SS via EPD. Determining the effect of PTFE particles incorporated in the PEEK/PTFE coating was essential. The average load was progressively increased from 5 to 7, 9, and 10 N on the sharp tip of the diamond indentor that scratched the coating. Visual observation showed that the scratch width remained constant from 5 N to 7 N. Still, a significant increase in the scratch width was observed at 9 N and 10 N, which indicated a critical failure point of the PEEK/PTFE coating at this level of load. It was concluded that the PEEK/PTFE coating can sustain a load of 7 N without any significant damage to the coating. In comparison, the PEEK coating delaminated at 5 N. Thus, the PEEK coating has an adhesion strength of 5 N. Figures 6, 7 show the digital images of scratch tests conducted to evaluate the adhesion strength of PEEK and PEEK/PTFE coatings deposited on 316L SS, respectively. The scratch resistance of the PEEK/PTFE coating is close to the values reported in the literature (Ur Rehman et al., 2017). The suitable adhesion strength of the PEEK/PTFE coatings can be attributed to the controlled heating/sintering temperature and deposition parameters.

3.6 Electrochemical studies

3.6.1 EIS analysis

The EIS data of 316L SS, PEEK coating, and PEEK/PTFE coating are represented in the form of Nyquist plots and Bode plots (Bode impedance plot and Bode phase angle plot) (Hernández et al., 2020). These data show the impedance response of a system (316L SS, PEEK coating, and PEEK/PTFE coating) to a small applied alternating current (AC) voltage. Figure 8 shows the curves that provide an insight into the corrosion mechanism and protective properties of PEEK and PEEK/PTFE coatings deposited on 316L SS via EPD. EIS data were analyzed using ZSimpWin software, which provided the quantitative approach to understanding the corrosion behavior of bare 316L SS, PEEK coating, and PEEK/PTFE coating in PBS.

Figure 8A shows the equivalent electrical circuit (EEC) used to describe the electrochemical behavior of 316L SS, PEEK coating, and PEEK/PTFE coating (Ahmad et al., 2023b; Minhas et al., 2020; Zhang et al., 2019). The solution resistance (Rs), charge transfer resistance (R_1), and coating resistance (R2), respectively. At the same time, the constant phase elements (Q_1) and (Q_2) described the capacitance of double layer and coatings, respectively (Zhang et al., 2019).

Nyquist plots show three capacitive arcs attributed to the 316L SS, PEEK coating, and PEEK/PTFE coating, as shown in Figure 8B. These capacitive arcs represent the impedance behavior of the 316L SS, PEEK coating, and PEEK/PTFE coating under a similar consistent corrosion condition under the PBS electrolyte. These capacitive arcs at the high-frequency range are related to charge transfer resistance (Minhas et al., 2020; Chaudry et al., 2022). The PEEK/PTFE coating exhibited enormous capacitive arcs than those related to the PEEK coating and bare 316L SS samples, which indicates the higher charge transfer resistance attributed to the PEEK/PTFE coating against the charge transportation

TABLE 3 Illustrates the PDP analysis using PBS for 316L SS, PEEK coating, and PEEK/PTFE coating deposited via EPD.

Substrate	Corrosion potential E_{corr} (V)	Corrosion rate (mpy)	Current density (A/cm^2)
316L SS	−0.264	0.943	31×10^{-7}
PEEK coating	−0.215	0.067	1.21×10^{-7}
PEEK/PTFE coating	−0.164	0.014	7.2×10^{-8}

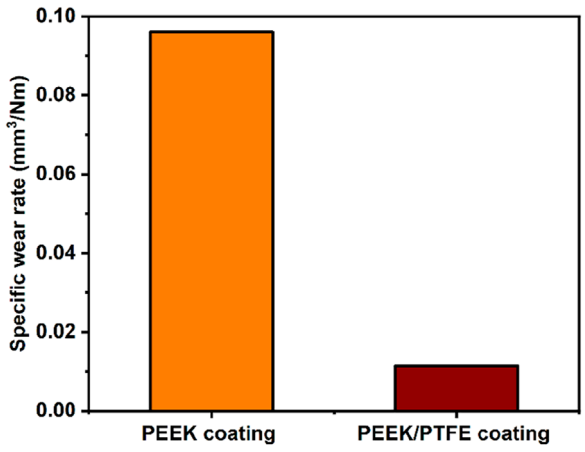

FIGURE 10
Shows the comparison between specific wear rates of PEEK and PEEK/PTFE coatings.

that may occur at a specific area of the electrode (PEEK/PTFE coating)/electrolyte (PBS) interface.

This indicates that the PEEK/PTFE coating has improved barrier properties compared to the PEEK coating and bare 316L SS substrates.

Bode impedance plots also provide an insight into the barrier properties of the oxide layer on 316L SS, PEEK coating, and PEEK/PTFE coating deposited on 316L SS. Their impedance behaviors are displayed as the modulus of impedance and phase angle, which are the functions of frequency (in log scale). Figure 8C describes the Bode impedance plots for 316L SS, PEEK coating, and PEEK/PTFE coating. However, PEEK and PEEK/PTFE coatings showed almost similar behavior at the whole frequency range by displaying a linear relationship between log(f) and log |Z|, demonstrating their capacitive behaviors. Still, this behavior was more prominent in the PEEK/PTFE coating than in the PEEK coating. However, the Bode impedance curve belonging to bare 316L SS showed resistive behavior at a high frequency range. The linear region of the frequency range for the PEEK/PTFE coating is more evident than that of the PEEK coating and bare 316L SS, which indicates the sound corrosion resistance of the PEEK/PTFE coating than that of the PEEK coating and bare 316L SS (Ahmad et al., 2023a; Minhas et al., 2020; De Riccardis et al., 2015).

Furthermore, the PEEK/PTFE coating exhibited a higher capacitive response in the higher frequency range, while showing a minimum value of phase angle than PEEK coating and bare 316L SS, which illustrated that the PEEK/PTFE coating exhibited higher insulating properties than those of the PEEK coating and bare 316L SS. Figure 8D shows the Bode phase angle plots of bare 316L SS, PEEK coating, and PEEK/PTFE coating. Table 2 shows that the charge transfer resistance (Rct) is much more excellent than the R1, implying that the charge transfer resistance dominates the overall protection to the corrosion resistance (Ahmad et al., 2023a; Minhas et al., 2020; Ahmad et al., 2023b; De Riccardis et al., 2015).

3.6.2 PDP analysis

The PDP analysis of 316L SS, PEEK coating, and PEEK/PTFE coating was carried out using the PBS solution, as shown in Figure 9. Tafel extrapolation was derived from the PDP curves of 316L SS, PEEK coating, and PEEK/PTFE coating. These data were analyzed in the corrosion view (CView) software, and the corrosion current density (i_{corr}), corrosion potential (E_{corr}), and corrosion rates (mills per year mpy) were calculated.

The PDP results after analysis showed that the PEEK/PTFE coating demonstrated superior corrosion resistance by exhibiting the lowest i_{corr} of ~ 7.2×10^{-8} A/cm^2, nobler corrosion potential of ~ − 0.164 V, and the slowest corrosion rate of ~0.0147 mpy as compared to the PEEK coating. Table 3 illustrates the concise and clear overview of the PDP-analyzed data of three samples. Moreover, after sintering at 350°C for 30 min, the PEEK coating demonstrated enhanced corrosion resistance when deposited on 316L SS, but the PEEK/PTFE coating further improved the corrosion resistance of 316L SS. This improvement in corrosion resistance is attributed to the incorporation of PTFE particles in the PEEK coating. It might be assumed that PTFE particles provided an additional dense barrier due to the infusion of PTFE particles due to sintering in the PEEK matrix. A combination of both PEEK and PTFE particles provided an effective barrier against the corrosive species of the bulk of the solution of PBS to reach the underlying 316L SS. A similar effect was observed by Corni et al. (2009) and Kumar et al. (2024).

3.6.3 Tribological study

PEEK and PEEK/PTFE coatings were subjected to the pin-on-disc tests. Both coatings showed stable behavior throughout a sliding distance of 30 m under a constant load of 7 N. Figure 10 compares the specific wear rates of PEEK and PEEK/PTFE coatings deposited on 316L SS via EPD. This stable behavior of the PEEK/PTFE coating throughout the sliding distance indicates that the PEEK/PTFE coating can maintain its frictional performance for extended times, making it a suitable candidate to improve the wear resistance of orthopedic implants [31].

The comparison between specific wear rates of PEEK and PEEK/PTFE coatings is shown in Figure 10 under the load of 7 N for a sliding distance of 30 m. Specific wear rates were calculated by calculating the cumulative wear volume and then divided by the product of the sliding distance and applied load. The specific wear rate of the PEEK coating (~0.0961 mm^3/Nm) was substantially higher than the specific wear rate (~0.0114 mm^3/Nm) of the PEEK/PTFE coating. These results of particular wear rates were in agreement with those of a previous study, which also demonstrated that the specific wear rate of PEEK decreased by incorporation of PTFE particles (Qu, 2019; Suh and Sin, 1981; Qu et al., 2016). This observation indicates that PEEK/PTFE exhibited the lowest specific wear rate. Figure 10 shows that the PEEK/PTFE coating exhibited superior wear resistance behavior compared to the PEEK coating, which is attributed to incorporation of PTFE particles in the PEEK coating. Incorporating PTFE may lower the wear rate of coatings deposited on orthopedic implants, thus increasing the life of an implant (Vail et al., 2011).

4 Conclusion

In this study, we compared the characteristics of PEEK and PEEK/PTFE coatings for biomedical applications. Improving the wear and corrosion properties of the 316L SS-based implants is essential. Thus, in context, we deposited PEEK/PTFE coatings on 316L SS via EPD and later sintered to achieve the densification of the coatings. SEM images distinguish between the morphology of the PEEK and PEEK/PTFE coating. PTFE was seen in the rounded form within the PEEK matrix. FTIR analysis confirmed the presence of PEEK and PTFE in the coating. PEEK/PTFE coatings demonstrated promising characteristics for adequate surface roughness and wettability for bone regeneration application. It was observed that the addition of PTFE improved the adhesion strength with the 316L SS substrate, as the adhesion strength of 7 N was observed for the PEEK/PTFE coating. Furthermore, wear studies were conducted to confirm that the addition of PTFE has improved the lubrication properties and wear resistance compared to those of the PEEK coating (the PEEK coating exhibited a specific wear rate of ~0.0961 mm^3/Nm, while the PEEK/PTFE coating exhibited a particular rate of wear of ~0.0114 mm^3/Nm). It is essential that the coating should exhibit strong wear resistance to prevent wear debris, which may cause inflammation at the site of implantation. The results of the adhesion strength and wear resistance confirmed that the PEEK/PTFE coating could sustain implantation load and is suitable for coating orthopedic implants. PEEK/PTFE coatings also exhibited significantly improved corrosion resistance compared to the 316L SS and PEEK. Thus, PEEK/PTFE coatings can act as a strong barrier and prevent the uncontrolled release of toxic ions from 316L SS substrates to the human body. Overall, PEEK/PTFE coatings exhibited suitable morphological, surface, mechanical, and electrochemical properties for orthopedic applications. However, in the future, it is suggested that detailed biological studies, including antibacterial, cell culture, biomarker, and *in vivo* studies, should be done to confirm the suitability of the PEEK/PTFE coatings for the intended application. In the future, an antibacterial agent can be added to the coatings to prevent biofilm formation.

Data availability statement

The original contributions presented in the study are included in the article/Supplementary Material; further inquiries can be directed to the corresponding author.

Author contributions

AI: investigation, methodology, and writing–original draft. RM: investigation, methodology, writing–original draft, and writing–review and editing. HA: investigation, methodology, and writing–review and editing. MU: conceptualization, investigation, methodology, project administration, visualization, and writing–review and editing.

Funding

The author(s) declare financial support was received for the research, authorship, and/or publication of this article. The authors extend their appreciation to Prince Sattam bin Abdulaziz University for funding this research work through the project number (2023/01/25861).

Conflict of interest

The authors declare that the research was conducted in the absence of any commercial or financial relationships that could be construed as a potential conflict of interest.

Publisher's note

All claims expressed in this article are solely those of the authors and do not necessarily represent those of their affiliated organizations, or those of the publisher, the editors, and the reviewers. Any product that may be evaluated in this article, or claim that may be made by its manufacturer, is not guaranteed or endorsed by the publisher.

References

Ahmad, K., Batool, S. A., Farooq, M. T., Minhas, B., Manzur, J., Yasir, M., et al. (2023a). Corrosion, surface, and tribological behavior of electrophoretically deposited polyether ether ketone coatings on 316L stainless steel for orthopedic applications. *J. Mech. Behav. Biomed. Mater.* 148, 106188. doi:10.1016/j.jmbbm.2023.106188

Ahmad, K., Manzur, J., Tahir, M., Hussain, R., Khan, M., Wadood, A., et al. (2023b). Electrophoretic deposition, microstructure and selected properties of zein/cloves coatings on 316L stainless steel. *Prog. Org. Coatings* 176, 107407. doi:10.1016/j.porgcoat.2023.107407

Ahmed, Y., Rehman, M. A. U., Ur Rehman, M. A., and Rehman, M. A. U. (2020). Improve the surface properties of stainless steel via zein/hydroxyapatite composite coatings for biomedical applications. *Surfaces Interfaces* 20, 100589. doi:10.1016/j.surfin.2020.100589

Ali, S., Irfan, M., Niazi, U. M., Rani, A. M. A., Rashedi, A., Rahman, S., et al. (2022). Microstructure and mechanical properties of modified 316L stainless steel alloy for biomedical applications using powder metallurgy. *Mater. (Basel)* 15, 2822. doi:10.3390/ma15082822

Armağan, M., and Arıcı, A. A. (2021). Investigation on fracture toughness of polytetrafluoroethylene with impact essential work of fracture method. *Polym. Polym. Compos.* 29, S335–S343. doi:10.1177/09673911211003392

Atiq, M., Rehman, U., Azeem, M., Schubert, D. W., Boccaccini, A. R., Rehman, M. A. U., et al. (2019). Electrophoretic deposition of chitosan/gelatin/bioactive glass composite coatings on 316L stainless steel: a design of experiment study. *Surf. Coatings Technol.* 358, 976–986. doi:10.1016/j.surfcoat.2018.12.013

Atiq Ur Rehman, M., Bastan, F. E., Haider, B., Boccaccini, A. R., Rehman, M. A. U., Bastan, F. E., et al. (2017). Electrophoretic deposition of PEEK/bioactive glass composite coatings for orthopedic implants: a design of experiments (DoE) study. *(DoE) study* 130, 223–230. doi:10.1016/j.matdes.2017.05.045

Atiq Ur Rehman, M., Chen, Q., Braem, A., Shaffer, M. S. P., and Boccaccini, A. R. (2020). Electrophoretic deposition of carbon nanotubes: recent progress and remaining challenges. *Int. Mater. Rev.* 66, 533–562. doi:10.1080/09506608.2020.1831299

Avcu, E., Baştan, F. E., Abdullah, H. Z., Rehman, M. A. U., Avcu, Y. Y., and Boccaccini, A. R. (2019). Electrophoretic deposition of chitosan-based composite coatings for biomedical applications: a review. *Prog. Mater. Sci.* 103, 69–108. doi:10.1016/j.pmatsci.2019.01.001

Avcu, E., Yasemin, Y., Erdem, F., Atiq, M., Rehman, U., Üstel, F., et al. (2018). Tailoring the surface characteristics of electrophoretically deposited chitosan-based bioactive glass composite coatings on titanium implants via grit blasting. *Prog. Org. Coatings* 123, 362–373. doi:10.1016/j.porgcoat.2018.07.021

Ballarre, J., Aydemir, T., Liverani, L., Roether, J. A., Goldmann, W. H., and Boccaccini, A. R. (2020). Versatile bioactive and antibacterial coating system based on silica, gentamicin, and chitosan: improving early stage performance of titanium implants. *Surf. Coatings Technol.* 381, 125138–138. doi:10.1016/j.surfcoat.2019.125138

Baştan, F. E., Rehman, M. A. U., Avcu, Y. Y., Avcu, E., Üstel, F., Boccaccini, A. R., et al. (2018). Electrophoretic co-deposition of PEEK-hydroxyapatite composite coatings for biomedical applications. *Colloids Surfaces B Biointerfaces* 169, 176–182. doi:10.1016/j.colsurfb.2018.05.005

Batool, S. A., Wadood, A., Hussain, S. W., Yasir, M., and Ur Rehman, M. A. (2021). A brief insight to the electrophoretic deposition of PEEK-chitosan-gelatin-and zein-based composite coatings for biomedical applications: recent developments and challenges. *Surfaces* 4, 205–239. doi:10.3390/surfaces4030018

Besra, L., and Liu, M. (2007). A review on fundamentals and applications of electrophoretic deposition (EPD). *Prog. Mater. Sci.* 52, 1–61. doi:10.1016/j.pmatsci.2006.07.001

Boccaccini, A. R., Keim, S., Ma, R., Li, Y., and Zhitomirsky, I. (2010). Electrophoretic deposition of biomaterials. *J. R. Soc. Interface* 7, S581–S613. doi:10.1098/rsif.2010.0156.focus

Celles, C. A. S., and dos Reis, A. C. (2024). Titanium: a systematic review of the relationship between crystallographic profile and cell adhesion. *J. Biomed. Mater. Res. Part B Appl. Biomater.* 112, e35450. doi:10.1002/jbm.b.35450

Chaudry, U. M., Farooq, A., Tayyab, K. bin, Malik, A., Kamran, M., Kim, J.-G., et al. (2022). Corrosion behavior of AZ31 magnesium alloy with calcium addition. *Corros. Sci.* 199, 110205. doi:10.1016/j.corsci.2022.110205

Chen, S., Chen, Y., Lei, Y., and Yin, Y. (2009). Novel strategy in enhancing stability and corrosion resistance for hydrophobic functional films on copper surfaces. *Electrochem. Commun.* 11, 1675–1679. doi:10.1016/j.elecom.2009.06.021

Chen, X., Ma, R., Min, J., Li, Z., Yu, P., and Yu, H. (2020). Effect of PEEK and PTFE coatings in fatigue performance of dental implant retaining screw joint: an *in vitro* study. *J. Mech. Behav. Biomed. Mater.* 103, 103530. doi:10.1016/j.jmbbm.2019.103530

Corni, I., Neumann, N., Novak, S., König, K., Veronesi, P., Chen, Q., et al. (2009). Electrophoretic deposition of PEEK-nano alumina composite coatings on stainless steel. *Surf. Coatings Technol.* 203, 1349–1359. doi:10.1016/j.surfcoat.2008.11.005

De Riccardis, M. F., Carbone, D., and Capodieci, L. (2015). Electrophoretically deposited polymeric films: evidence of correlation between electrochemical impedance spectroscopy measurements and morphological properties. *J. Electrochem. Soc.* 162, D3071–D3076. doi:10.1149/2.0201511jes

De Riccardis, M. F., Martina, V., and Carbone, D. (2013). Study of polymer particles suspensions for electrophoretic deposition. *J. Phys. Chem. B* 117, 1592–1599. doi:10.1021/jp3051752

de Sá, M. D., de Lima Souza, J. W., da Silva, H. N., Torres, R. H. N., Leite, M. D. R., Barbosa, R. C., et al. (2021). Biocompatible sulphonated PEEK spheres: influence of processing conditions on morphology and swelling behavior. *Polym. (Basel)* 13, 2920. doi:10.3390/polym13172920

Dhanumalayan, E., and Joshi, G. M. (2018). Performance properties and applications of polytetrafluoroethylene (PTFE)—a review. *Adv. Compos. Hybrid. Mater.* 1, 247–268. doi:10.1007/s42114-018-0023-8

Ferrari, B., and Moreno, R. (2010). EPD kinetics: a review. *J. Eur. Ceram. Soc.* 30, 1069–1078. doi:10.1016/j.jeurceramsoc.2009.08.022

Fiołek, A., Zimowski, S., Kopia, A., Łukaszczyk, A., and Moskalewicz, T. (2020a). Electrophoretic Co-deposition of polyetheretherketone and graphite particles: microstructure, electrochemical corrosion resistance, and coating adhesion to a titanium alloy. *Mater. (Basel)* 13, 3251. doi:10.3390/ma13153251

Fiołek, A., Zimowski, S., Kopia, A., Sitarz, M., and Moskalewicz, T. (2020b). Effect of low-friction composite polymer coatings fabricated by electrophoretic deposition and heat treatment on the Ti-6Al-4V Titanium Alloy's tribological properties. *Metall. Mater. Trans. A* 51, 4786–4798. doi:10.1007/s11661-020-05900-3

Heavens, S. N. (1990). Electrophoretic deposition as a processing route for ceramics. *Noyes Publ. Adv. Ceram. Process. Technol.* 1, 255–283.

Hernández, H. H., Reynoso, A. M. R., González, J. C. T., Morán, C. O. G., Hernández, J. G. M., Ruiz, A. M., et al. (2020). "Electrochemical impedance spectroscopy (EIS): a review study of basic aspects of the corrosion mechanism applied to steels," in *Electrochemical impedance spectroscopy*. Editors M. El-Azazy, M. Min, and P. Annus (Rijeka: IntechOpen). Ch. 1. doi:10.5772/intechopen.94470

Kumar, A. M., Ogunlakin, N., Al Dahwali, F., and Saji, V. S. (2024). Electrophoretically deposited PEEK/PDMS composite coatings for 316L SS bioimplants. *Mater. Lett.* 354, 135375. doi:10.1016/j.matlet.2023.135375

Mahmoud Nasef, M., Saidi, H., Ahmad, A., and Ahmad Ali, A. (2013). Optimization and kinetics of phosphoric acid doping of poly(1-vinylimidazole)-graft-poly(ethylene-co-tetrafluorethylene) proton conducting membrane precursors. *J. Memb. Sci.* 446, 422–432. doi:10.1016/j.memsci.2013.05.053

Matsuura, T., Komatsu, K., Cheng, J., Park, G., and Ogawa, T. (2024). Beyond microroughness: novel approaches to navigate osteoblast activity on implant surfaces. *Int. J. Implant Dent.* 10, 35. doi:10.1186/s40729-024-00554-x

Minhas, B., Dino, S., Qian, H., and Zuo, Y. (2020). An approach for high stability TiO2 in strong acid environments at high temperature. *Surf. Coatings Technol.* 395, 125932. doi:10.1016/j.surfcoat.2020.125932

Moskalewicz, T., Seuss, S., and Boccaccini, A. R. (2013). Microstructure and properties of composite polyetheretherketone/Bioglass® coatings deposited on Ti–6Al–7Nb alloy for medical applications. *Appl. Surf. Sci.* 273, 62–67. doi:10.1016/j.apsusc.2013.01.174

Moskalewicz, T., Zimowski, S., Zych, A., Łukaszczyk, A., Reczyńska, K., and Pamuła, E. (2018). Electrophoretic deposition, microstructure and selected properties of composite alumina/polyetheretherketone coatings on the Ti-13Nb-13Zr alloy. *J. Electrochem. Soc.* 165, D116–D128. doi:10.1149/2.0681803jes

Nawaz, A., Bano, S., Yasir, M., Wadood, A., Ur Rehman, M. A., and Rehman, M. A. U. (2020). Ag and Mn-doped mesoporous bioactive glass nanoparticles incorporated into the chitosan/gelatin coatings deposited on PEEK/bioactive glass layers for favorable osteogenic differentiation and antibacterial activity. *Mater. Adv.* 1, 1273–1284. doi:10.1039/D0MA00325E

Nawaz, M. H., Aizaz, A., Ropari, A. Q., Shafique, H., Imran, O. bin, Minhas, B. Z., et al. (2023). A study on the effect of bioactive glass and hydroxyapatite-loaded Xanthan dialdehyde-based composite coatings for potential orthopedic applications. *Sci. Rep.* 13, 17842. doi:10.1038/s41598-023-44870-5

Nawaz, M. H., Aizaz, A., Shafique, H., Ropari, A. Q., bin Imran, O., Abbas, M., et al. (2024). Rosemary loaded Xanthan coatings on surgical grade stainless steel for potential orthopedic applications. *Prog. Org. Coatings* 186, 107987. doi:10.1016/j.porgcoat.2023.107987

Nawaz, Q., Fastner, S., Rehman, M. A. U., Ferraris, S., Perero, S., di Confiengo, G. G., et al. (2021). Multifunctional stratified composite coatings by electrophoretic deposition and RF co-sputtering for orthopaedic implants. *J. Mater. Sci.* 56, 7920–7935. doi:10.1007/s10853-020-05725-w

Panayotov, I. V., Orti, V., Cuisinier, F., and Yachouh, J. (2016). Polyetheretherketone (PEEK) for medical applications. *J. Mater. Sci. Mater. Med.* 27, 118. doi:10.1007/s10856-016-5731-4

Pishbin, F., Mouriño, V., Flor, S., Kreppel, S., Salih, V., Ryan, M. P., et al. (2014). Electrophoretic deposition of gentamicin-loaded bioactive glass/chitosan composite coatings for orthopaedic implants. *ACS Appl. Mater. Interfaces* 6, 8796–8806. doi:10.1021/am5014166

Pishbin, F., Mouriño, V., Gilchrist, J. B. B., McComb, D. W. W., Kreppel, S., Salih, V., et al. (2013). Single-step electrochemical deposition of antimicrobial orthopaedic coatings based on a bioactive glass/chitosan/nano-silver composite system. *Acta Biomater.* 9, 7469–7479. doi:10.1016/j.actbio.2013.03.006

Qu, S. (2019). Tribology of PTFE/PEEK composite at elevated temperature.

Qu, S., Penaranda, J., and Wang, S. S. (2016). "Tribological behavior of PTFE/PEEK composite," in *Technical conference*.

Rehman, M. A. U., and Batool, S. A. (2022). Development of sustainable antibacterial coatings based on electrophoretic deposition of multilayers: gentamicin-loaded chitosan/gelatin/bioactive glass deposition on PEEK/bioactive glass layer. *Int. J. Adv. Manuf. Technol.* 120, 3885–3900. doi:10.1007/s00170-022-09024-3

Simchi, A., Tamjid, E., Pishbin, F., Boccaccini, A. R., Simchi, A., Tamjid, E., et al. (2011). Recent progress in inorganic and composite coatings with bactericidal capability for orthopaedic applications. *Nanomedicine Nanotechnol. Biol. Med.* 7, 22–39. doi:10.1016/j.nano.2010.10.005

Song, J., Liao, Z., Wang, S., Liu, Y., Liu, W., and Tyagi, R. (2016). Study on the tribological behaviors of different PEEK composite coatings for Use as Artificial Cervical Disk materials. *J. Mater. Eng. Perform.* 25, 116–129. doi:10.1007/s11665-015-1842-1

Suh, N. P., and Sin, H.-C. (1981). The genesis of friction. *Wear* 69, 91–114. doi:10.1016/0043-1648(81)90315-x

Ureña, J., Tsipas, S., Jiménez-Morales, A., Gordo, E., Detsch, R., and Boccaccini, A. R. (2018). Cellular behaviour of bone marrow stromal cells on modified Ti-Nb surfaces. *Mater. Des.* 140, 452–459. doi:10.1016/j.matdes.2017.12.006

Ur Rehman, M. A., Bastan, F. E., Nawaz, A., Nawaz, Q., Wadood, A., Rehman, M. A. U., et al. (2020). Electrophoretic deposition of PEEK/bioactive glass composite coatings on stainless steel for orthopedic applications: an optimization for *in vitro* bioactivity and adhesion strength. *Int. J. Adv. Manuf. Technol.* 108, 1849–1862. doi:10.1007/s00170-020-05456-x

Ur Rehman, M. A., Ferraris, S., Goldmann, W. H., Perero, S., Bastan, F. E., Nawaz, Q., et al. (2017). Antibacterial and bioactive coatings based on radio frequency Co-sputtering of silver nanocluster-silica coatings on PEEK/bioactive glass layers obtained by electrophoretic deposition. *ACS Appl. Mater. Interfaces* 9, 32489–32497. doi:10.1021/acsami.7b08646

Vail, J. R., Krick, B. A., Marchman, K. R., and Sawyer, W. G. (2011). Polytetrafluoroethylene (PTFE) fiber-reinforced polyetheretherketone (PEEK) composites. *Wear* 270, 737–741. doi:10.1016/j.wear.2010.12.003

Wang, H., Wen, Y., Peng, H., Zheng, C., Li, Y., Wang, S., et al. (2018). Grafting polytetrafluoroethylene micropowder via *in situ* electron beam irradiation-induced polymerization. *Polym. (Basel)* 10, 503. doi:10.3390/polym10050503

Wang, P., Zhang, D., Qiu, R., Wu, J., and Wan, Y. (2013). Super-hydrophobic film prepared on zinc and its effect on corrosion in simulated marine atmosphere. *Corros. Sci.* 69, 23–30. doi:10.1016/j.corsci.2012.10.025

Wennerberg, A. (1999). The role of surface roughness for implant incorporation in bone. *Cells Mater* 9, 1–19.

Xiang, Q., Qin, J., Qin, T., Chen, L., and Zhang, D. (2022). Kinetics study of anodic electrophoretic deposition for polytetrafluoroethylene (PTFE) coatings on AZ31 magnesium alloy. *BMC Chem.* 16, 92. doi:10.1186/s13065-022-00884-0

Xu, Y., Gao, D., Dong, Q., Li, M., Liu, A., Wang, X., et al. (2021). Anticorrosive behavior of epoxy coating modified with hydrophobic nano-silica on phosphatized carbon steel. *Prog. Org. Coatings* 151, 106051. doi:10.1016/j.porgcoat.2020.106051

Yuan, X.-D., and Yang, X.-J. (2010). A study on friction and wear properties of PTFE coatings under vacuum conditions. *Wear* 269, 291–297. doi:10.1016/j.wear.2010.04.014

Zhang, D., Zhuo, L., and Xiang, Q. (2023a). Electrophoretic deposition of polytetrafluoroethylene (PTFE) as anti-corrosion coatings. *Mater. Lett.* 346, 134524. doi:10.1016/j.matlet.2023.134524

Zhang, J., Zhang, X., Liu, Z., Zhang, L., Zhao, Y., Li, Y., et al. (2023b). Study on preparation and anticorrosive performance of a new high hydrophobic anticorrosive coating. *J. Appl. Polym. Sci.* 140, e53459. doi:10.1002/app.53459

Zhang, Y., Luo, H., Zhong, Q., Yu, H., and Lv, J. (2019). Characterization of passive films formed on as-received and sensitized AISI 304 stainless steel. *Chin. J. Mech. Eng.* 32, 27–12. doi:10.1186/s10033-019-0336-8